

FSSCAT MISSION DESCRIPTION AND FIRST SCIENTIFIC RESULTS OF THE FMPL-2 ONBOARD ³CAT-5/A

A. Camps^{1,2}, J.F. Munoz-Martin¹, J.A. Ruiz-de-Azua^{1,2}, L. Fernandez¹, A. Perez-Portero¹, D. Llavería¹, C. Herbert¹, M. Pablos³, A. Golkar^{4,1}, A. Gutiérrez⁵, C. António⁵, J. Bandejas⁵, J. Andrade⁵, D. Cordeiro⁵, S. Briatore^{4,6}, N. Garzaniti^{4,6}, F. Nichele⁷, R. Mozzillo⁷, A. Piumatti⁷, M. Cardi⁷, M. Esposito⁸, B. Carnicero Dominguez⁹, M. Pastena⁹, G. Filippazzo¹⁰, A. Reagan¹⁰

¹Universitat Politècnica de Catalunya, Barcelona, Spain;

²Institut d'Estudis Espacials de Catalunya, Barcelona, Spain,

³Institut de Ciències del Mar (ICM-CSIC) & Barcelona Expert Center (BEC) on Remote Sensing, Barcelona, Spain;

⁴Skolkovo Institute of Science and Technology, Moscow, Russia;

⁵Deimos Eng., Lisbon, Portugal,

⁶Golbriak Space, Tallin, Estonia;

⁷Tyvak International, Torino, Italy;

⁸Cosine, Oostende, The Netherlands;

⁹ESA ESTEC, Noordwijk, The Netherlands;

¹⁰ESA ESRN, Frascati, Italy.

E-mail: camps@tsc.upc.edu

ABSTRACT

FSSCat, the “Federated Satellite Systems/³Cat-5” mission was the winner of the 2017 ESA S³ (Sentinel Small Satellite) Challenge and overall winner of the Copernicus Masters competition. FSSCat consists of two 6 unit cubesats carrying on board UPC's Flexible Microwave Payload – 2 (FMPL-2), an L-band microwave radiometer and GNSS-Reflectometer implemented in a software defined radio, and Cosine's HyperScout-2 visible and near infrared + thermal infrared hyperspectral imager, enhanced with PhiSat-1, a on board Artificial intelligence experiment for cloud detection. Both spacecrafts include optical and UHF inter-satellite links technology demonstrators, provided by Gölbriak Space and UPC, respectively. This paper describes the mission, and the main scientific results of the FMPL-2 obtained during the first three months of the mission, notably the sea ice concentration and thickness, and the downscaled soil moisture products over the Northern hemisphere.

Index Terms— Microwave Radiometry, GNSS-R, sea ice concentration, sea ice thickness, soil moisture, artificial neural networks.

1. INTRODUCTION

The FSSCat mission was proposed in 2017 by Prof. Camps (UPC) and Prof. Golkar (Skoltech, UPC visiting professor) the ESA S³ (Sentinel Small Satellite) Challenge of the Copernicus Masters competition. FSSCat is an innovative mission consisting of two federated 6U Cubesats carrying two scientific payloads:

- UPC's Flexible Microwave Payload – 2 (FMPL-2) [1] onboard ³Cat-5/A (2020-061W) is an innovative dual

microwave payload (L-band microwave radiometer and GNSS-Reflectometer) implemented in a software defined radio,

- Cosine's HyperScout-2 [2] onboard ³Cat-5/B (2020-061X) is an hyper-spectral optical payload in the visible, near and thermal infrared, enhanced with PhiSat-1 [3] an [Artificial Intelligence experiment](#) for cloud detection.

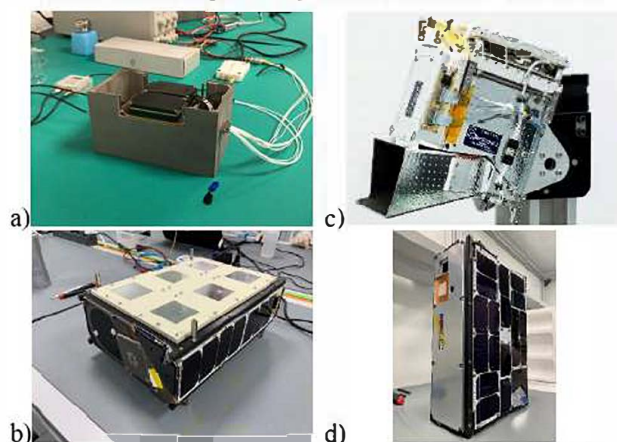


Fig. 1. a) FMPL-2 combined microwave radiometer and GNSS-reflectometer, b) ³Cat-5/A and dual-band nadir looking antenna, c) HyperScout-2, and d) ³Cat-5/B with HyperScout-2 baffle on the bottom right corner.

The mission goals of ³Cat-5/A are to provide coarse resolution soil moisture, sea ice extent and thickness maps, and to detect water ponds over ice, using microwave radiometry and GNSS-Reflectometry, enhanced resolution soil moisture maps applying pixel downscaling techniques, and to test techniques for future satellite federations. FSSCat

could be a precursor of a scalable constellation of federated small Earth Observation satellites.

In addition to UPC (ES) and Cosine (NL), the scientific payload providers, the implementation of this challenging mission in approximately 1.5 years, was conducted by a team including Golbriak Space (EE), provider of the Optical Inter-satellite link, Deimos Engenharia (PT), prime contractor and responsible for the Data Processing Ground Segment, Tyvak International (IT), platform provider, system integrator, Cubesat deployer provider and launch interface, and operations manager, and ESA EOP which initiated the ESA Sentinel Small Satellite Challenge, provided technical and programmatic advise and expertise, the funding scheme, and access to ESA testing facilities.

1.1. Scientific Rationale

FSSCat targets two main scientific goals: sea ice and snow monitoring in polar regions, and surface soil moisture using L-band microwave radiometry and GNSS-R, as at present there is no follow-on mission for either SMOS or SMAP, although the Copernicus Imaging Microwave Radiometers (CIMR) includes an L-band channel, and two Chinese missions have been recently approved. Regarding sea ice, L-band microwave radiometry can be used to infer sea ice thickness up to ~60 cm [4]. On the other hand, GNSS-R is very sensitive to the surface where the scattering is taking place. Figure 2 shows the measurement principle of GNSS-R. For altimetry/scatterometry applications the information is in the differential delay/power between the reflected and direct signals. GNSS-R is sensitive to both the peak and the shape of the Delay Doppler Map (DDM), or the cross-correlation of the reflected signal with a locally-generated replica of the transmitted one for different Doppler frequencies and delay bins [5], as illustrated in Fig. 3. Regarding soil moisture, validated algorithms have been developed to downscale SMOS-derived products using VNIR data, as shown in Fig. 4 using [6].

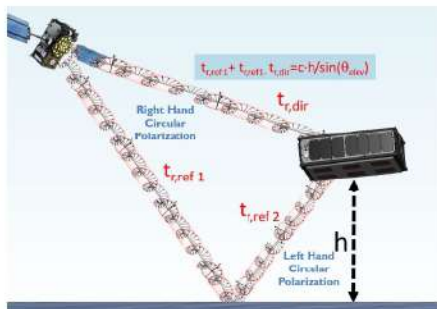


Fig. 2. Measurement principle of GNSS-R.

1.2. Data Acquisition Strategy

FMPL-2 acquires data in blocks of 100 ms split into 40 ms for the GNSS-R processor and 100 ms for the microwave radiometer. Radiometer data are delivered at 2 Hz, and up to 2 or 4 GNSS-R specular reflections per second at 40 ms integration time can be produced for Galileo or GPS.

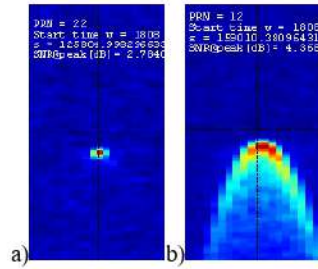


Fig. 3. TDS-1 GNSS-R Delay Doppler Maps obtained over a) ice, and b) ocean.

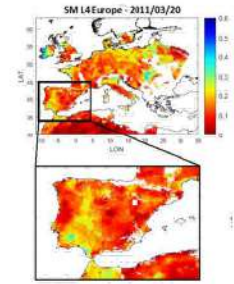


Fig. 4. Sample downscaled Soil Moisture Map over Europe obtained at the BEC.

In order to achieve the best possible spatial resolution for sea ice extent detection, the integration time was selected to be 40 ms so that the blurring due to the speed of the subsatellite point equals the size of the first Fresnel zone (Fig. 5a). The 100 ms integration time for the microwave radiometer leads to a radiometric sensitivity low-enough to compensate for the wind speed effects of the brightness temperatures over the ocean.

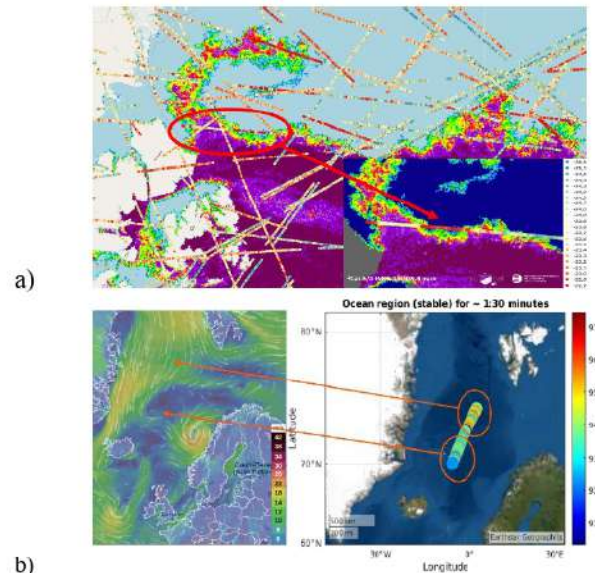


Fig. 5. a) Sample FMPL-2 DDM peak SNR over ice, b) Sample brightness temperature over the South Pacific

In orbit, FMPL-2 is executed over the poles following a 5-day basis: 5 days in a row over the North Pole at latitudes >55° (after ~1 month it was set to 45°, and finally 35°), and 5 days in a row over the South Pole at latitudes < -55°.

³Cat-5/A data is downloaded at the UPC ground station located in the Observatori Astronòmic del Montsec, owned and operated by the IEEC (Fig. 6). The ground station consists of an S-Band 3-meter dish with a G/T = 9dB, and operating from 2200-2290 MHz. There is also a pair of antennas at VHF and UHF operating in the radio-amateur bands. The second one (435-438 MHz) is used for the FSS Experiment.



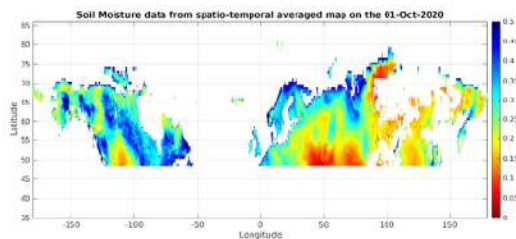
Fig. 6. VHF/UHF-bands Yagi antennas (left) and S-band dish (right) UPC ground station at IEEC's Observatori Astronòmic del Montsec where ³Cat-5/A data is downloaded.

2. SCIENTIFIC DATA PROCESSING

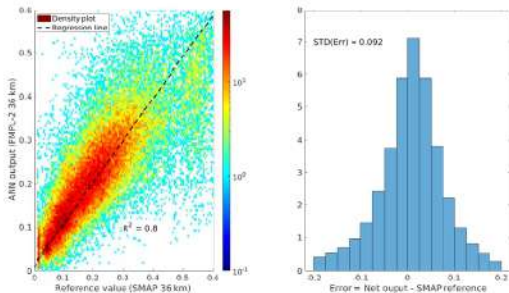
The three scientific products listed above have been processed using Artificial Neural Networks (ANN) that have been trained using a suite of input variables (different for each product), and “the ground truth” as the output.

2.1. Soil Moisture

Soil Moisture is derived from the combination of the land surface temperature (ECMWF ERA 5 skin temperature, 30 km resolution), multispectral images (notably the red and near infra-red channels, or the NDVI from NASA MODIS, 1 km spatial resolution), and the FMPL-2 L-band brightness temperatures (circular polarization at nadir, footprint size 350 x 500 km²). The ANN is a 2-hidden layer feed-forward network with 7 neurons each. To avoid overfitting, it is trained with 60% of the data using SMAP 36 km soil moisture product, and the training is interrupted at 20 epochs. Figure 7a shows a sample soil moisture map produced over a week. Figure 7b shows the scatter plot of the soil SMAP moisture values and the FMPL-2/ANN retrieved ones. As it can be appreciated, the $R^2 = 0.8$ and the standard deviation of the error with respect to the SMAP product is about 9.2%.



a)



b)

Fig. 7. a) Weekly average soil moisture map derived from FMPL-2 using an ANN, and b) error statistics.

2.2. Sea Ice Concentration and Extent

Sea ice concentration (SIC) maps can be generated using SAR and visible sensors, but SAR processing is very demanding, and has poorer coverage than microwave radiometers. Sea ice extent (SIE) maps are derived from SIC maps by thresholding.

For the SIC/SIE retrievals two different ANNs have been used: a regression fit ANN for SIC with 3 hidden layers and 5, 10 and 5 neurons each, and for SIE a binary classification ANN with a single hidden layer with 10 neurons. These networks have been trained using OSI SAF [7] or NSIDC ground truth as a target output, and the FMPL-2 brightness temperature, the ERA 5 skin temperature, and the land cover (%) as input variables. Figure 8 shows sample SIE (top) and SIC (bottom) maps for the Arctic and Antarctica, as derived from FMPL-2.

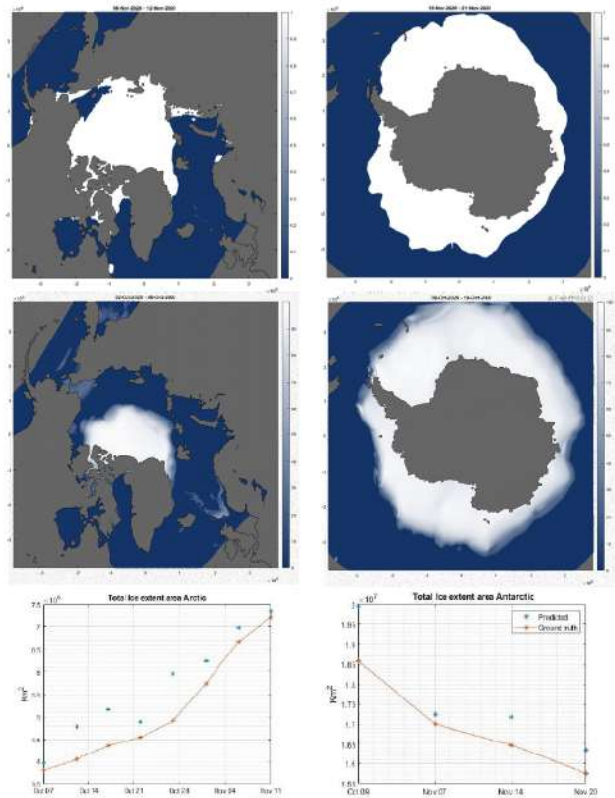


Fig. 8. Sample SIE (top) and SIC (center) maps for the Arctic and Antarctica, as derived from FMPL-2, and temporal evolution during October and November. Error is < 6% when compared to OSI SAF “ground truth”

As it can be expected by inspection of Figs. 3 and 5a, SIE can also be derived from GNSS-R retrievals with improved spatial resolution, and in particular using ANNs. As in the microwave radiometer case, a pattern recognition network is used, trained with OSI SAF ground truth data, and using as inputs: the FMPL-2 GNSS-R derived DDM, reflectivity, and SNR, the elevation and azimuth, and the brightness

temperature. Figure 9 shows two examples to illustrate that GNSS-R can differentiate water from ice, and different types of ice, at a much higher resolution than the antenna footprint. The expected error is less than 5% when compared to OSI SAF.

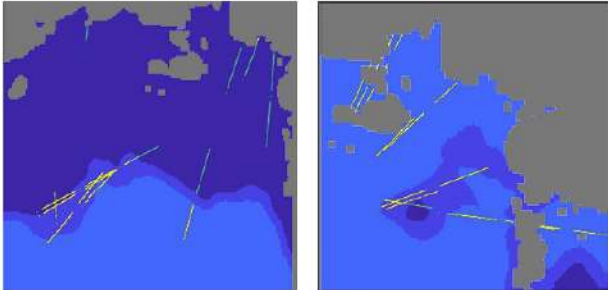


Fig. 9. Two examples of GNSS-R tracks classifying water (green) from ice (yellow). Error is < 5% when compared to OSI SAF “ground truth”

2.3. Sea Ice Thickness

Sea Ice Thickness is derived from the combination of three input variables: the FMPL-2 microwave radiometer data, ECMWF ERA 5 skin temperature, and OSI SAF OSI-401-b SIC product. The training output variable is the daily Sea-Ice Thickness from SMOS, which is used as “ground truth.” The implemented algorithm is a predictive regression model - Deep Neural Network (DNN) with one normalization layer, two hidden dense non-linear layers (64 neurons), and one linear single-output layer.

Figure 10 presents some sample results for the a) Arctic, and b) Antarctica, as well as the associated error metrics: c) the scatter plot of the SMOS-derived SIT used as a ground truth and the FMPL-2/DNN-predicted SIT showing a good agreement up to 40-50 cm SIT with a small standard deviation, and d) the Mean Absolute Error (MAE) histogram, showing a nearly unbiased SIT prediction with a standard deviation of 6.5 cm.

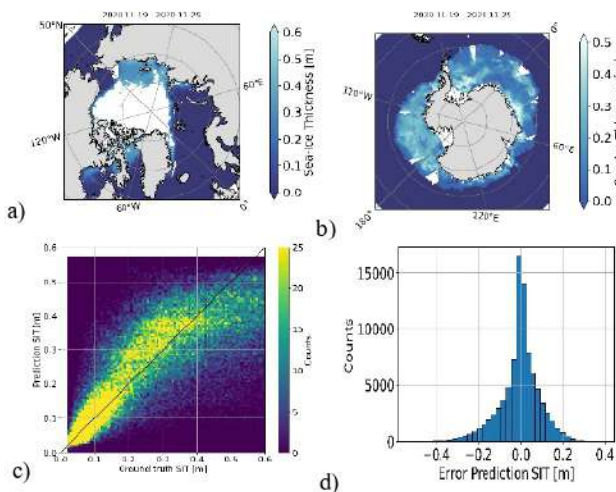


Fig. 10. Sample SIT maps over a) the Arctic, b) Antarctica, and error statistics: c) SMOS SIT ground truth/FMPL-2 DNN SIT scatter plot and d) MAE histogram.

3. CONCLUSIONS

This paper has presented the main results of the FMPL-2 combined (microwave radiometer and GNSS-R payload onboard ³Cat-5/A of the FSSCat mission during the first three months of operations for sea ice concentration/extent and thickness and soil moisture.

FFSCat has been possible in a record time (1.5 year + 1 year launch delay due to VV15 explosion and covid-19) thanks to a committed team bringing their best to a common objective: to show the potential of small satellites to conduct valuable scientific missions, or as gap-fillers while waiting for larger and more performant missions to be launched. One can also envisage a not-so-distant future where constellations of small satellites carrying state-of-the-art Earth Observation intelligent and interconnected payloads form a network that provides global near real-time data that could be ingested by the digital models of the Earth’s climate.

4. ACKNOWLEDGMENTS

This work was supported by 2017 ESA S³ challenge and Copernicus Masters overall winner award (“FSSCat” project) and ESA project “FSSCat Validation Experiment in MOSAIC”, by the Spanish Ministry of Science, Innovation and Universities, “Sensing with Pioneering Opportunistic Techniques” SPOT, grant RTI2018-099008-BC21/AEI/10.13039/501100011033, and by the Unidad de Excelencia Maria de Maeztu MDM-2016-0600.

5. REFERENCES

- [1] J. F. Muñoz-Martin, L. F. Capon, J. A. Ruiz-de-Azua and A. Camps, “The Flexible Microwave Payload-2: A SDR-Based GNSS-Reflectometer and L-Band Radiometer for CubeSats,” in *IEEE Journal of Selected Topics in Applied Earth Observations and Remote Sensing*, vol. 13, pp. 1298-1311, 2020, doi: 10.1109/JSTARS.2020.2977959.
- [2] HyperScout-2: <https://www.cosine.nl/cases/hyperscout-2/> (last visited, December 31st, 2020)
- [3] M. Pastena, B. Camicero Dominguez, P.P. Matthieu et al. “ESA Earth Observation Directorate NewSpace initiatives” Small Satellite Conference Utah State University 2019 SSC19-V-05
- [4] L. Kaleschke, et al., “SMOS sea ice product: operational application and validation in the Barents Sea marginal ice zone”. *Remote Sensing of Environment* 180. (2016): S. 264-273.
- [5] A. Alonso-Arroyo, V. U. Zavorotny and A. Camps, “Sea Ice Detection Using U.K. TDS-1 GNSS-R Data,” *IEEE Transactions on Geoscience and Remote Sensing*, vol. 55, no. 9, pp. 4989-5001, Sept. 2017
- [6] G. Portal et al., “A Spatially Consistent Downscaling Approach for SMOS Using an Adaptive Moving Window,” in *IEEE Journal of Selected Topics in Applied Earth Observations and Remote Sensing*, vol. 11, no. 6, pp. 1883-1894, June 2018, doi: 10.1109/JSTARS.2018.2832447.
- [7] OSI SAF Sea Ice Concentration (SSMIS): <http://www.osi-saf.org/?q=content/global-sea-ice-concentration-ssmis> (last visited, December 31st, 2020)